Void Shape in Gas-Channel Ribs in Gas-Assisted Injection-Molded Plates

S. Y. YANG and P. T. CHU

Department of Mechanical Engineering, National Taiwan University, Taipei, Taiwan, ROC

Received: March 5, 1998
Accepted: September 8, 1998

ABSTRACT: Large, thin, plate-shaped parts are usually strengthened with structural ribs. Ribs also serve as gas channels with gas-assisted technology. Gas penetration in the gas channels results in improved moldability and also eliminates sink marks and prevents warpage. However, gas leaves the rib core void, which degrades rigidity. This study examines the shape of the gas void and its relation to rib geometry and processing conditions. The effects of rib geometry, including aspect ratio and fillet geometry, along with processing conditions such as delay time, melt temperature, gas pressure and characteristics of the GAIM molded parts on void shapes are investigated. Numerical simulation of temperature distribution in the rib area is used to aid interpretations of gas void shapes. © 1999 John Wiley & Sons, Inc. Adv Polym Techn 18: 11–17, 1999

Introduction

Large, thin, plate-shaped parts are usually strengthened with ribs. With gas-assisted technology, gas penetration into the gas channels improves moldability, eliminates sink marks, and prevents warpage. However, gas leaves the rib core void, which degrades rigidity. Further complicating matters, the shape and distribution of the gas void depends on processing conditions. Gas void size, shape, and distribution are especially sensitive to rib geometry and processing conditions.

For designers, estimation of rigidity-degrading effects is a critical step for optimal design. Available literature on gas-assisted injection molding is mostly general or introductory,[1—5] or theoretical.[6–9] Zheng et al.[10] and Findeisen[11] carried out analytical and experimental studies on gas-assisted injection molding, but they did not focus on fundamental rib design. Baxi[12] suggested several proven rib shapes for GAIM molds, and Chen et al.[13] attempted to simulate the melt front advancement during the filling of a plate cavity with a rib of semicircular cross-section. Poslinski et al.[14] per-

Correspondence to: S. Yang

CCC 0730-6679/99/010011-07

formed isothermal gas-assisted displacement of viscoplastic liquids in tubes in which the wall thicknesses around the cores were found set by the solid skin and a thick molten layer. These aforementioned analyses have not systematically covered most rib geometry.

Yang et al.[15] systematically investigated the effect of rib geometry, including aspect ratio and fillet geometry, on GAIM. They found that increasing the rib width widens the allowable operation range and thus improves the moldability. Adding fillets, especially curved ones, to the rib corners significantly enhances the moldability and improves rigidity. However, the gas void shape and its relation to rib geometry and processing conditions (such as melt temperature, gas pressure, delay time, etc.) have not been investigated adequately. Better grasp of the factors determining formation of void shape is essential to enhance the capacity of applying gas-assisted technology to molding.

The present study examines gas void and its relation to rib geometry and processing conditions: rib geometry includes aspect ratio and fillet profile; and processing conditions include melt temperature, gas pressure, and gas injection delay. The shape and position of the void formed in the rib section with various rib geometries and processing conditions are studied. Temperature distributions at various timepoints in the rib section are simulated with finite-element software. They are employed to aid in interpreting the void shapes observed in sliced cross-sections.

Experimental Setup

Gas-assisted injection molding experiments were conducted with a 50-ton injection molding machine (Polypax, GG50, Taiwan). A lab-made gas injection unit was attached to the machine. The gas injection system consisted of a nitrogen tank, pressure regulators, valves, a solenoid, and a controller for gas-injection delay control.[15] The gas pressure was regulated with a pressure regulator (TKR-100, Japan). When the valve was opened by the solenoid, the gas with regulated pressure was injected through the injection needles in the cavity. Timing was controlled by the signal from the controller. A counter circuit was triggered by the melt-injection signal from the injection molding machine. After a preset delay, a DC voltage was applied to the solid-state relay. The solenoid then opened the valve to the gas injection needle.

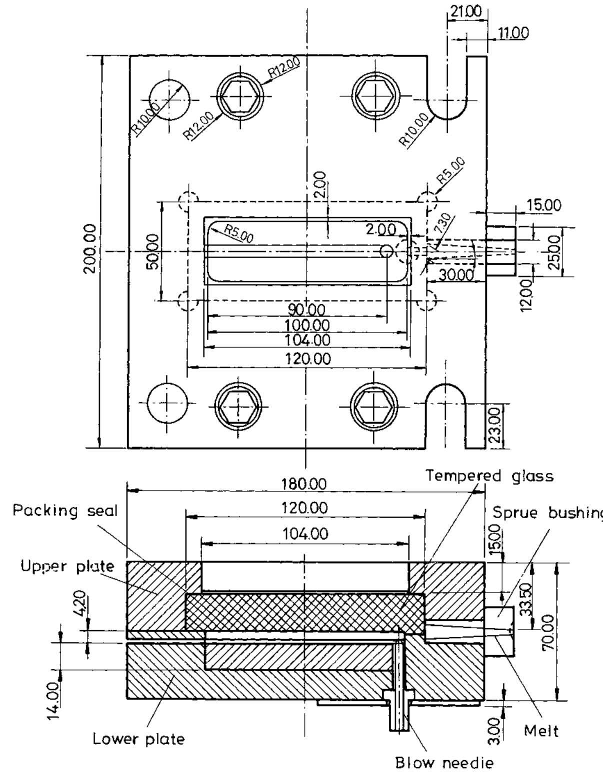

FIGURE 1. Construction of the mold for GAIM experiments with glass windows for flow visualization.

The mold is composed of two plates (Fig. 1) clamped vertically between the platens of the machine. A thick tempered-glass window with rubber sealing was mounted on the upper plate to allow for flow visualization. The cavity bottom-piece is

TABLE I
Rib with Different Aspect Ratios and Fillet Shapes

Ribs	Aspect Ratio (W/t)	Fillet
A1	0.5	None
A2	1.0	None
A3	1.5	None
A4	2.0	None
B1	0.5	Straight
B2	1.0	Straight
B3	1.5	Straight
B4	2.0	Straight
C1	0.5	Circular
C2	1.0	Circular

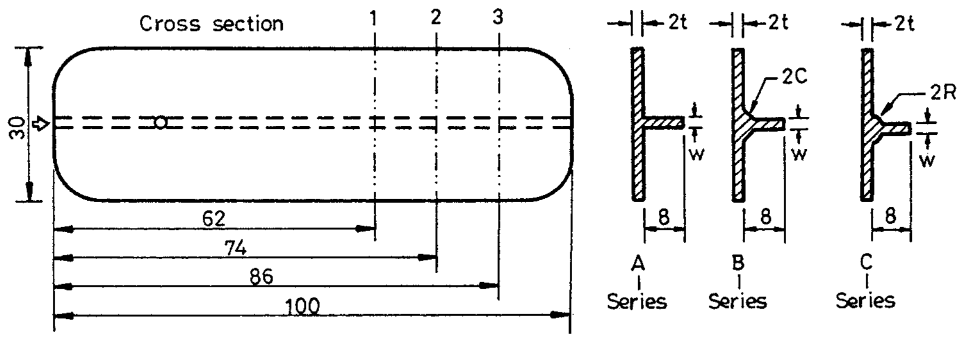

FIGURE 2. Schematic of the molded parts with different rib shapes (series A, rib without fillet; series B, rib with 45° straight fillet; series C, rib with circular fillet).

seated on the lower plate. The bottom-piece is exchanged for molding parts with different rib shapes. The part geometry for three types of ribs (i.e., ribs without fillet and ribs with straight and circular fillets) are shown in Figure 2. A-series ribs are of typical rectangular shape. B-series ribs are rectangular ribs filleted with 45° edges at transitional corners. C-series ribs are rectangular ribs with circular fillets at transitional corners. A summary of the rib types with the width-to-thickness aspect ratios (w/t) used in this experiment is given in Table I.

Because these rib shapes are combined from basic geometry, a second set of molds was constructed to further analyze the contribution of these basic geometrical components to moldability and rigidity. This second set of mold a U-shaped cavity to lengthen the flow path as shown in Figure 3. The rib cross-sections are rectangular (R), circular (C), and trapezoidal (T) in shape. For the ribs of basic geometry, the cross-sectional area and the height of each rib are designed to be nearly the same. Injection-grade polystyrene PG-79 (Chi-Mei, Taiwan) was used in this study. The molding conditions employed were: maximum time for filling: 8 sec; injection speed and pressure (stage 1): 40%, 30%; injection speed and pressure (stage 2): 40%, 30%; rear zone setpoint temperature: 205°C; front zone setpoint temperature: 220°; delay time after short-shot filling: 0.5 sec; gas pressure: 60 kg/cm^2.

The shape of the rib, along with the size and shape of the gas void, has a crucial effect on the part rigidity. For the ribs of basic geometry (from the second set of molds), the cross-sectional area and the height of each rib are designed to be nearly the same. The rigidities can then be evaluated directly based on the maximum bending strength in a three-point bending test. Because the cross-sectional areas of the ribs of different aspect ratios and fillet shapes are not the same, the rigidity of parts molded from the first set of molds cannot be evaluated directly

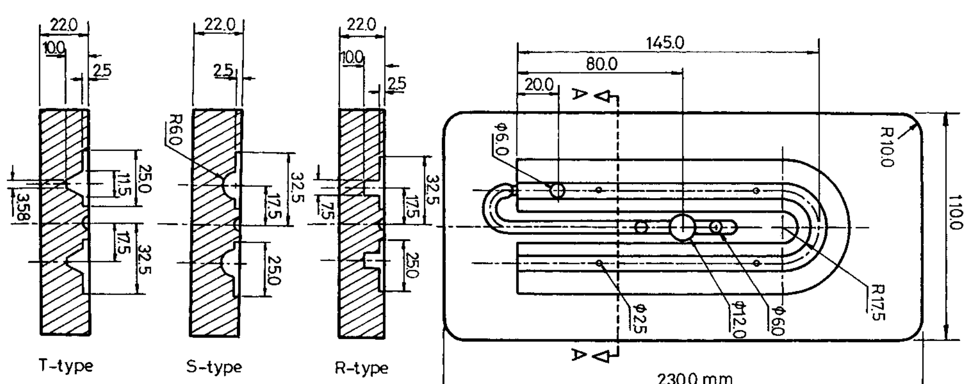

FIGURE 3. Schematic showing the mold of U-shaped plates with ribs of basic geometry (type R: rectangular; type S: semicircular; type T: trapezoidal).

TABLE II
Material Properties Used in Numerical Simulation

Material	Density (kg/cm³)	Conductivity (W/m K)	Heat Capacity (J/kg K)
PS	970 (220°C), 1021 (110°C)	0.4368	1260
Mold	7800	54.0	465
Glass	2500	0.8	672

with bending resistance. Only the shape and the location of gas voids are observed and are used indirectly to predict the degree of weakening.

Numerical Model

Temperature distribution and evolution in the rib region are computed using finite-element analysis. A plate with a rib in a steel mold with a glass window is modeled as a two-dimensional heat conduction problem. The material properties used are shown in Table II. Meshing is designed to render the best efficiency with limited resources. Finite-element software, ANSYS (AISI, USA), is used to simulate heat transfer evolution and temperature distribution in rib sections.

Results and Discussion

VOID SHAPE IN RIBS WITH DIFFERENT WIDTH AND SHAPE

A typical cross-section with gas void in plates with rectangular ribs without and with straight and circular fillets is shown in Figure 4. Two distinct void sizes are observed: large and small. Near the far end of the plates (area 3 in Fig. 2), all voids are comparatively small and round in shape. They are formed during postfilling, namely gas-assisted packing and cooling. During postfilling, the solidifying polymer undergoes volumetric shrinkage, allowing gas to penetrate further into the parts for purposes of compensation. The small and round voids are formed by shrinkage-induced gas penetration, or secondary gas penetration. Conceivably, the shape of the gas voids with shrinkage-induced gas penetration is more predictable. The following discussion is focused on flow-induced gas penetration, so-called primary penetration, which occurs during gas-assisted filling. The shapes of large voids, formed by primary penetration, depend on the aspect ratio and fillet profile. For rectangular ribs without fillets, triangular gas voids with large height-to-base ratios are formed near the rib roots. For ribs with 45° straight fillets, voids of equilateral triangular shape are formed. For ribs with circular fillets, voids of semicircular shape are formed. The skin thickness at the transitional corner is most uniform with circular fillets.

The temperature distributions in the plates with different rib width and shape are shown in Figure 5. For the extremely narrow rib (A1, w/t 0.5), all temperatures are below the glass transition temperature after delay, and the gas cannot even blow in during primary penetration. The temperatures in the plates with a wider rib (w/t > 1), the isotherms in the core show an area with temperatures higher than T_g. The gas can penetrate along this high-temperature core. The shape of the gas voids are thus observed, as shown in Figure 4. Temperature distribution plays an important role in determining the void shapes of gas-assisted injection molded parts.

To further investigate the relation between void

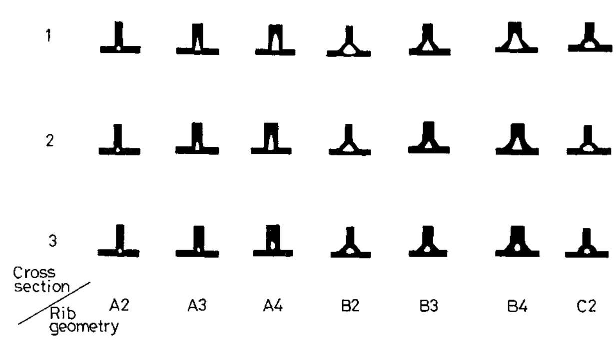

FIGURE 4. Sectional views showing the gas void shapes at selected locations of gas-assisted molded parts with different aspect ratios and fillet shapes. The locations of sections 1, 2, and 3 for observing gas voids are indicated in Figure 2.

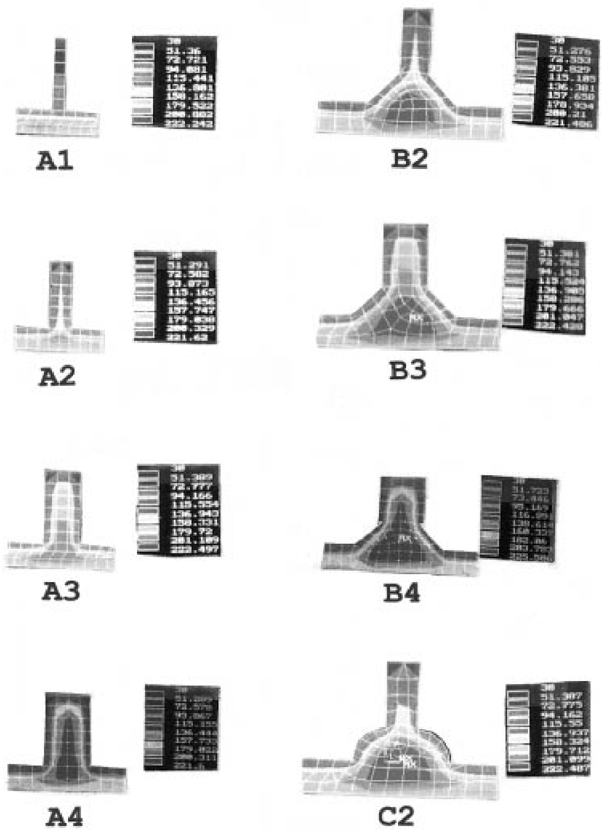

FIGURE 5. The temperature distribution in plates with ribs of different width and shape (1.5 sec after injection).

shape and temperature distribution, ribs with same width, but different shape (A4, B4, and C4), were molded with different gas injection delay times. The cross-sectional view is shown in Figure 6, along with simulated temperature distribution. The longer delay time increases the frozen layer thickness and reduces the void sizes. Basically, the void geometry resembles the isotherms. However, the isotherm may contain sharp edges, whereas the gas void looks much smoother due to a surface tension effect. As the gas-injection delay time increases, the area of gas void decreases and the shape becomes more circular.

VOID SHAPE IN RIBS OF BASIC GEOMETRY

The temperature distribution in ribs along with a void shape of basic geometry (circular, trapezoid, rectangular) is shown in Figure 7. Due to the simplicity of the rib geometry, the isotherms take up the shape of the rib and the void shape is close to

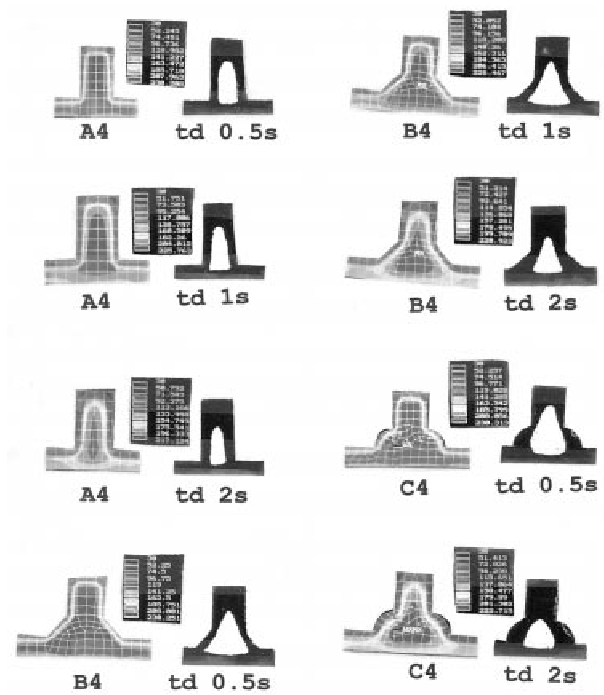

FIGURE 6. The temperature distribution and gas void shape in plates with ribs of the same width, but different shape, molded with various gas injection delays.

the shape of the isotherms. For comparison, a step-type rib is also displayed. The isotherms are much different from the geometry boundary due to the sharp edges.

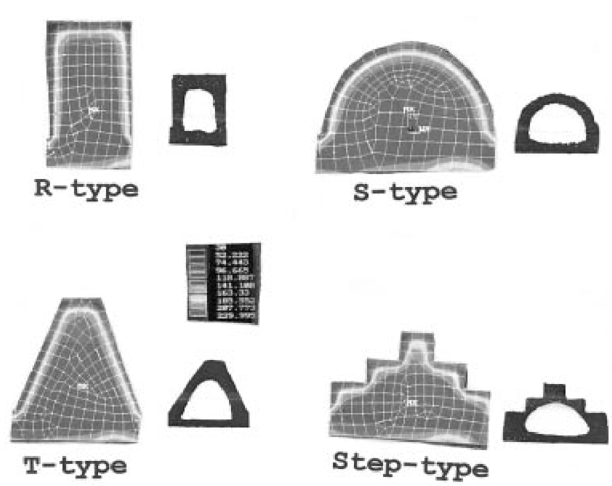

FIGURE 7. The temperature distribution and gas void shape in plates with ribs of basic geometry (1.0 sec after injection).

EFFECTS OF SHORT SHOT, GAS PRESSURE, AND MELT TEMPERATURE ON VOID SHAPE

The void shapes in Figure 8 display the effects of short-shot size and gas injection pressure. The temperature distribution is shown in Figure 7. A smaller short-shot results in longer penetration length and smaller void area. With the same short shot, higher gas pressure results in larger void size. Figure 9 shows the void shapes with different melt temperatures (along with temperature distribution). Higher melt temperature enlarges the area of high temperature core and thus the area of gas void. However, the effects are not evident.

EFFECTS OF VOID AREA ON RIGIDITY

The void areas and bending strength of a series of plates with circular, trapezoidal, and rectangular ribs (GAIM molded at different melt temperature, gas pressure, and short shot) are shown in Table III. As can be seen, the rectangular rib shows the best bending resistance, and the circular rib the poorest.

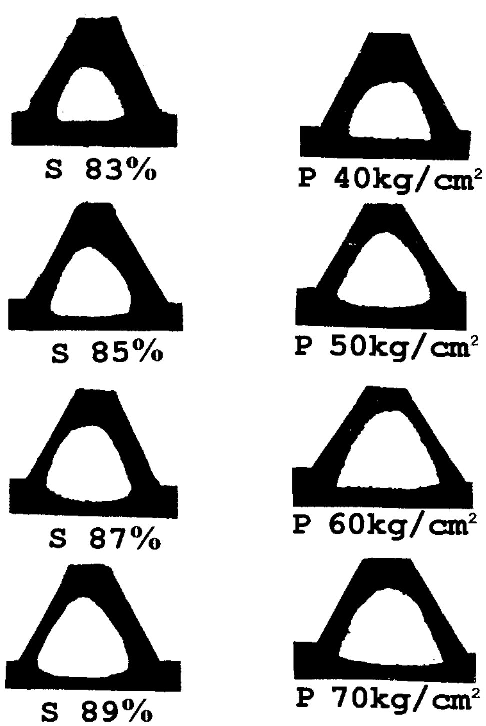

FIGURE 8. The gas void shape in plates with trapezoid ribs molded with different short shot and gas pressure.

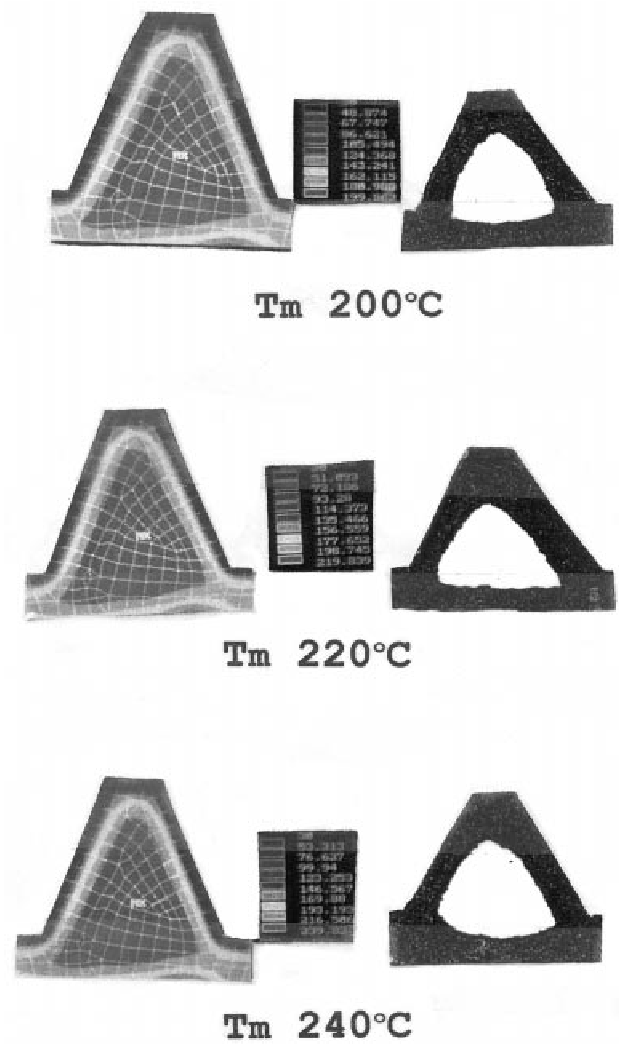

FIGURE 9. The temperature distribution and gas void shape in plates with trapezoid ribs molded with different melt temperatures.

Summary and Conclusions

The shape of the gas void with different rib geometries under various processing conditions was investigated in this work. Rib geometry included width-to-part thickness and shape of transitional fillets. Ribs of three basic geometries were also examined. Results of numerical simulations of the temperature distribution in the rib region at different timepoints were also provided to determine the relationship between void shape and thermal conditions.

TABLE III
Bending Strength of Parts with Ribs of Basic Geometry

Geometry	T_m (°C)	P_{gas} (kg/cm^2)	Short Shot (%)	Void (%)	$S_{bending}$ (N/mm^2)
Semicircular	210	50	77.1	25.3	3.72
Semicircular	210	80	74.7	25.9	3.67
Semicircular	250	50	73.7	27.0	3.61
Semicircular	250	80	72.2	27.3	3.57
Trapezoid	210	50	77.9	24.2	4.18
Trapezoid	210	80	76.8	25.1	4.14
Trapezoid	250	50	76.1	26.2	4.06
Trapezoid	250	80	74.9	26.9	4.05
Rectangular	210	50	80.5	21.2	4.74
Rectangular	210	80	78.7	21.1	4.61
Rectangular	250	50	78.8	25.9	4.55
Rectangular	250	80	77.6	23.4	4.47

The following conclusions can be drawn from this study:

1. Voids formed during secondary penetration (during postfilling) are small and circular in shape. Voids formed during primary penetration (during gas-assisted filling) are large, and the shape depends on the rib geometry and processing conditions. Triangular voids with high height-to-base ratios are formed with nonfilleted rectangular ribs. Equilateral triangular voids are formed with filled ribs.
2. Basically, void geometry resembles that of isotherms. However, the isotherm may contain sharp edges, whereas the gas void appears much smoother due to a surface tension effect. As the gas-injection delay time increases, the area of gas void decreases and the shape becomes more circular. The addition of transitional fillets substantially smoothens the isotherms. Adding transitional fillets also smoothens the shape of the gas void.
3. The void shapes are additionally determined by processing conditions. Short-shot size shows the most significant effect. Less short shot size results in longer primary gas penetration length and smaller void size. High gas pressure and melt temperature increase the void size.

References

1. Fallows, W. J. Plast Engng 1982, 12, 27.
2. Bernhardt, R. Engng Plast 1992, 5, 397.
3. Menges, G. Int Polym Sci Technol 1991, 18, 40.
4. Rusch, K. C. SPE ANTEC Tech Papers 1989, 1014.
5. Shah, S.; Hlavaty, D. SPE ANTEC Tech Papers 1991, 1479.
6. Potente, H.; Hensen, M. Int Polym Proc 1993, 8, 345.
7. Turng, L. S. Adv Polym Technol 1995, 14, 1.
8. Chen, S. C.; Cheng, N. T.; Hsu, K. S. Int Commun Heat Mass Transfer 1995, 22, 319.
9. Khayat, R.; Derdouri, A.; Hebert A. J Non-Newtonian Fluid Mech 1995, 57, 253.
10. Zheng, T.; Koskey, T.; Altan, T. SME Tech Papers CM93-416 1993.
11. Findeisen, H. PhD Dissertation, IKV, Germany 1994.
12. Baxi, I. SPI Annu Conf Struct Div 1990,18, 158.
13. Chen, S. C.; Hsu, K. F.; Hsu, K. S. Numer Heat Transfer 1995, 28, 121.
14. Poslinski, A. J.; Oehler, P. R.; Stokes, V. H. Polym Eng Sci 1995, 35, 877.
15. Yang, S. Y.; Huang, F. Z.; Liau, W. N. Polym Eng Sci 1996, 36, 2824.